International Journal of Power Electronics and Drive System (IJPEDS)
Vol. 7, No. 2, June 2016, pp. 481~497
ISSN: 2088-8694

Low Voltage Ride-through for Doubly Fed Induction Generator Using Battery-Storage System

D.V.N. Ananth*, G.V. Nagesh Kumar**
* Electrical Engineering Department, VITAM College of Engineering, Visakapatnam, India
** Electrical Department, GITAM UNIVERSITY, Visakapatnam, India

Article Info

Article history:

Received Dec 11, 2015
Revised Mar 31, 2015
Accepted Apr 10, 2016

Keyword:

DFIG
Field oriented control
Low voltage fault ride through
Voltage mitigation
Voltage sag

ABSTRACT

In this paper, enhanced field oriented control technique (EFOC) was adopted in Rotor Side Control (RSC) of DFIG converter for improved response during severe faults. The work is intended to damp pulsations in electromagnetic torque, improve voltage mitigation and limit surge currents and to enhance the operation of DFIG during voltage sags. The converter topology uses a battery energy storage system with capacitor storage system to further enhance operation of DFIG during faults. The battery and capacitor system in coordination provide additional real and reactive power support during faults and nearly constant voltage profile at stator and rotor terminals and limit overcurrents. For EFOC technique, rotor flux reference changes its value from synchronous speed to zero during fault for injecting current at the rotor slip frequency. In this process DC-Offset component of flux is controlled, decomposition during overvoltage faults. The offset decomposition of flux will be oscillatory in a conventional FOC, whereas in EFOC it will damp quickly. A comparison is made with proposed methodology with battery energy storage system and a conventional system. Later the system performance with under voltage of 50% the rated voltage with fault at PCC during 0.8 to 1.2 seconds is analysed using simulation studies.

Corresponding Author:

G.V. Nagesh Kumar,
Departement of Electrical and Electronics Engineering,
GITAM University, Visakapatnam, India.
Email: drgvnk14@gmail.com

1. INTRODUCTION

The doubly fed induction generator (DFIG) is having better preference due to its small size with higher MVA ratings available in the market, low power ratings of converters, variable generator speed and constant frequency operation, robust four quadrant reactive power control and much better performance during the low voltage ride through (LVRT). However, DFIG is sensitive to external disturbances like voltage swell and sag. If grid voltage falls or rises suddenly due to any reason, large surge currents enter into the rotor terminals and voltage induces significantly. Hence, the rotor side converter (RSC) will get damaged due to exceeding voltage or the current rating. Apart from this, there will be huge electromagnetic torque pulsations and increase in rotor speed which may reduce gears of the wind turbine-generator lifetime.

The status of research on the LVRT issue for DFIG for symmetrical and asymmetrical faults and comparison of different control strategies is given in [1]. Understanding the capability of RSC to deliver desired reactive power and withstanding capability during fault in [2]. In this paper, if the stator and rotor voltages are dropped to a certain value during fault, the DFIG turbine system got synchronized quickly after fault cleared and is made to operate as in pre-fault state. The paper aimed in smoothening of electromagnetic torque (EMT), and to control the reactive power to grid during fault time. Enhanced reactive power support [3], controlling DC link current of RSC to smoothen DC voltage fluctuations due to grid faults by using

stored Kinetic Energy [4] are techniques used to improve DFIG operation during LVRT. In these papers an additional reactive power support can enhance performance of DFIG system during sudden fault issues. Also crowbar as passive and RSC strategy as active compensation for LVRT reactive power compensation [5], FFTC scheme with PIR [6] and PI [7] with symmetrical and asymmetrical faults for improving uninterrupted P, Q supply from WT to grid and enhancement based on flux trajectory [8],. In these papers authors claim that, instead of using a conventional PI controller, PI + Resonant controller can perform better during asymmetrical faults for DFIG system. Few intelligent control techniques like Genetic Algorithm [9] and bacterial search etc were used in control strategies for improving the performance during LVRT and can improve voltage and current levels during fault and makes system more sustainable during and after fault. Some external passive elements and active sources are used in coordination for improving stability and thereby providing a better LVRT operation of DFIG during symmetrical and asymmetrical faults. Among external devices which were connected in coordination with DFIG system to enhance system LVRT behavior during severe faults is Single phase crowbar [11], Super-capacitor energy storage system [12], Fault Current Limiter (FCL) [13], Superconducting FCL with Magnetic Energy storage devices [14] were used recently. Therefore to control over current during severe faults, conventional crowbar circuit is avoided which disable DFIG to provide reactive power support throwing the grid into more critical state. From these papers, active energy storage devices are much helpful for rapid real and reactive power compensation for stator and rotor terminals with improved stability during symmetrical or asymmetrical faults.

A conventional vector control techniques in RSC does not provide low magnitude rotor over currents. They may trigger crowbar, pushing wind system to demand reactive power. With Enhanced Flux Oriented Control (EFOC) better reduction in rotor over currents can be made possible by considering the effect of direct axis stator flux ϕ_{ds} aligned with rotating stator flux. The BESS is used for controlling power fluctuations in the wind generation system [15-18], voltage and frequency fluctuations with reduced noise and vibration with BESS for isolated asynchronous generators is used in [19, 20]. A BESS based on multi-level PWM inverter for continuous and improved state of charging is proposed in [21, 22]. In [22], PSO based MIWP model is proposed to mitigate output power fluctuations in wind farm. The equivalent circuit for lithium ion based BESS is analysed and experimentally verified in [23].

As far as the storage technique is concerned, BESS is chosen for its cost effectiveness whereas Super Magnetic Energy Storage system is considerably cost and fly wheel [24], [25] takes large time constant to provide dynamic support to overall wind turbine system [9]. STATCOM with EFOC technique is used for different faults [26] for the enhancement in the performance of DFIG. Real and reactive power control is proposed in [27] for DFIG as per grid requirement. The performance of DFIG wind energy conversion system is compared with PI, ANN and hybrid PI and ANN in [28]. A hybrid PI and ANN controller for DFIG is examined in [28] to rapidly changing grid voltage conditions. The authors found that, active and reactive powers are having surges and also rotor and stator parameters got disturbed much with PI and their effects are low with ANN. However when using both PI and ANN, the effects said above got minimized and hence the authors in [19] conclude that hybrid is better control when grid voltage conditions are high. Also independent control of active and reactive power examined in this paper and found that fuzzy controller is better than conventional PI controller [29]. The authors compared the performance of DFIG during three phase to ground when controlled using PI and fuzzy. It is found that with fuzzy, stator and rotor voltage, current and power waveforms are better and have better stability than a conventional PI controller. The fuzzy controller is having faster control action and accurate performance due to faster changing disturbances. Predictive direct power control technique is applied to DFIG system in [30] to have quicker and robust performance to maintain constant DC link voltage with lesser harmonic current and for operation during sub synchronous and super- synchronous speed operation. Drooping characteristics of DFIG is studied in [31] and found that DFIG output power is controlled according to varying wind speed.

The present paper describes how (LVRT) behavior is achieved without sacrificing dynamic stability of DFIG system using an advanced control technique Enhanced Flux Oriented Control (EFOC) with aid of effective energy storage system connected through bidirectional switches to the dc link. This supports voltage at dc link and improves dynamic stability during symmetrical grid disturbances. This paper describes comparison between without BESS and with BESS to the DC link during symmetrical and asymmetrical voltage disturbances at grid. It also explains how efficiently a rotor current can be controlled with flux oriented mechanism.

In the section 2 describes the design of RSC for EFOC. Section 3 gives modelling under transient conditions was explained with symmetrical faults and design of EFOC for the LVRT issue is described. Further sections 4 describe the simulation results when a fault occurs at PCC with 50% decrease in the rated voltage. The efficacy of the proposed method is tested in the MATLAB environment and the conclusion are given in section 5 followed by appendix and references.

2. DESIGN OF ROTOR SIDE CONVERTER CONTROL FOR EFOC

RSC controller helps in improving reactive power demand at gris and to extract maximum power from the machine by making the rotor to run at optimal speed. The optimal speed of the rotor is decided from machine real power and rotor speed characteristic curves from MPPT algorithm. The stator active and reactive power control is possible with the RSC controller strategy through i_{qr} and i_{dr} components controlling respectively. The rotor voltage in a stationary reference frame [11] and further analysis from our paper [26] is given by

$$V_r^s = V_{0r}^s + R_r i_r^s + \sigma L_r \frac{di_r^s}{dt} - j\omega\, i_r^s \tag{1a}$$

with $\sigma = 1 - \frac{L_{sm}^2}{L_s L_r}$ and

ω is the rotor speed, i_r^s is the rotor current in a stationary frame of reference, Ls, Lr and Lm are stator, the rotor and mutual inductance parameters in Henry or in pu

$$V_{0r}^s = \frac{L_m}{L_s}\left(\frac{d}{dt} - j\omega_s\right)\Phi_s^s \tag{1b}$$

is the voltage induced in the stator flux with

$$\Phi_s^s = L_s i_s^s + L_m i_s^s \tag{2}$$

$$\Phi_r^s = L_r i_r^s + L_m i_r^s \tag{3}$$

The d and q axis rotor voltage equations (1a, 1b), (2) and (3) in the synchronous rotating reference frame are given by

$$V_{dr} = \frac{d\Phi_{dr}}{dt} - (\omega_s - \omega)\Phi_{qr} + R_r i_{dr} \tag{4}$$

$$V_{qr} = \frac{d\Phi_{qr}}{dt} - (\omega_s - \omega)\Phi_{dr} + R_r i_{qr} \tag{5}$$

The stator and rotor two axis fluxes are

$$\Phi_{dr} = (L_{lr} + L_m) i_{dr} + L_m i_{ds} \tag{6}$$

$$\Phi_{qr} = (L_{lr} + L_m) i_{qr} + L_m i_{qs} \tag{7}$$

$$\Phi_{ds} = (L_{ls} + L_m) i_{ds} + L_m i_{dr} \tag{8}$$

$$\Phi_{qs} = (L_{ls} + L_m) i_{qs} + L_m i_{qr} \tag{9}$$

where, $L_r = L_{lr} + L_m, L_s = L_{ls} + L_m, \omega_r = \omega_s - \omega$

By substituting (6), (7), (8), (9) in (4), (5) and by rearranging the terms, then

$$V_{dr} = \left(R_r + \frac{dL_r'}{dt}\right) i_{dr} - s\omega_s L_r' i_{qr} + \frac{L_m}{L_s} V_{ds} \tag{10}$$

$$V_{qr} = \left(R_r + \frac{dL_r'}{dt}\right) i_{qr} - s\omega_s L_r' i_{dr} + \frac{L_m}{L_s}(V_{qs} - \omega\Phi_{ds}) \tag{11}$$

Where ω is rotor speed, $\omega_{\Phi s}$ is speed of stator flux, ω_s is synchronous speed.

The MATLAB/ SIMULINK based on the control circuit of RSC for enhancing performance for LVRT issues are shown in Figure 1a, GSC converter in Figure 1b. The right side corner subsystem 2 is a sub-circuit of the controller for EFOC is shown later in Figure 3.

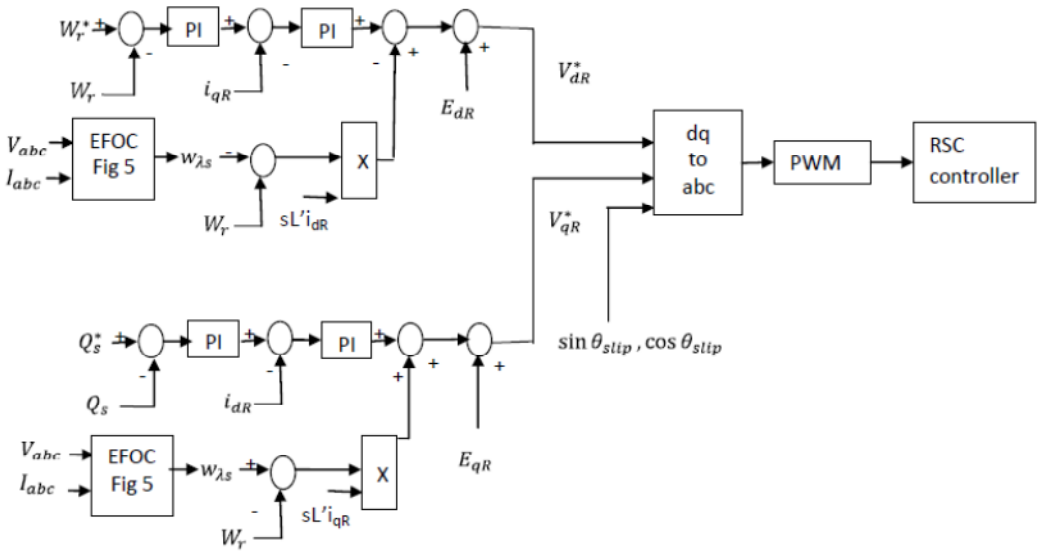

(a)

Figure 1a. The RSC controller with EFOC technique design for Grid connected DFIG with $E_{dR} = \frac{-L_m}{L_s}(V_{qS} + \lambda_{dR}\omega_r)$ and $E_{qR} = \frac{L_m}{L_s}V_{qS}$

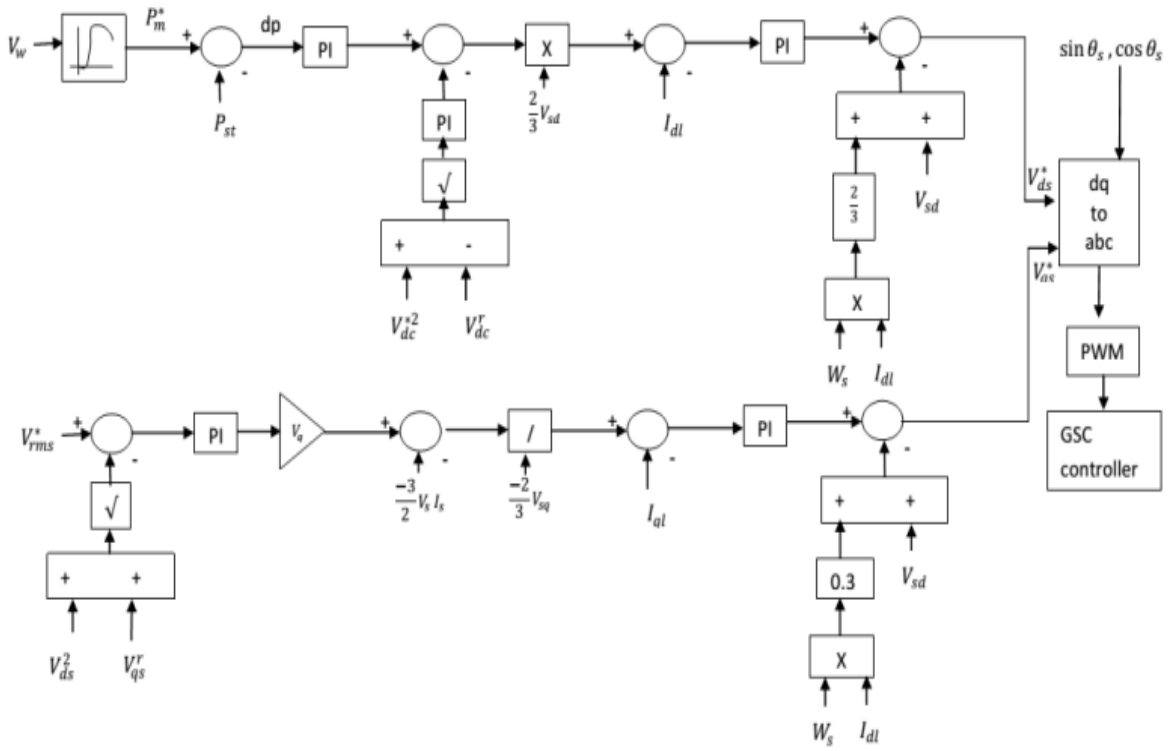

(b)

Figure 1b. Grid side controller for DFIG

The above equations 10 and 11 can be rewritten in terms of decoupled parameters and are designed for RSC controller as in equations 12 and 13.

$$\sigma V_{dr} = \sigma L_r \frac{dI_{dr}}{dt} - \omega_s \Phi_{qr} + \frac{L_m}{L_s}(V_{ds} - R_s I_{ds} + \omega_1 \Phi_{qs}) \quad (12)$$

$$\sigma V_{qr} = \sigma L_r \frac{dI_{qr}}{dt} - \omega_s \Phi_{dr} - \frac{L_m}{L_s}(R_s I_{qs} + \omega_1 \Phi_{ds}) \quad (13)$$

In general the rotor speed ω_r is and the synchronous speed of stator is ω_s.But this synchronous frequency has to be changed from ω_s to a new synchronous speed value as described in flowchart in Figure 3 ω_s' as it is represented commonly by ω_1. Under ideal conditions, reference stator d-axis flux Φ_d^* is zero and q-axis flux Φ_q^* is equal to the magnitude of stator flux $\Phi_s$for given back emf and rotor speed.

The GSC converter is shown in Figure 1b. the reference real power is extracted from lookup table based on wind speed. The error in this reference to actual power is controlled using PI controller. The difference in square of DC reference voltage to actual DC voltage is controlled using a tuned PI controller. The difference in the above two PI controllers and multiplied with stator d-axis current vector to get reference d-axis stator current. This current and actual stator output current is maintained to zero using PI controller. Using decoupling voltage vector control method, referenced-axis decoupled voltage will be extracted. In the similar way q-axis decoupled voltage vector is obtained. The d and q axis voltages are converted to 3 phase by using inverse park's transformation and further given to PWM to get pulses to the grid side converter circuit.

The flux derivation technique helps in understanding the operation of DFIG during steady state and transient state. The accuracy of system performance during steady state depends on accuracy of wind speed measurement action of the pitch angle controller, measurement of stator current, voltage, flux and other important parameters. The more accurate these measurements, the more can be a real power extracted from the DFIG wind turbine system. The equations 14 to 17 plays a vital role in understanding the behavior of DFIG during steady state and accuracy of RSC control action depends on control of the d and q axis voltages.

3. MATHEMATICAL ANALYSIS OF RSC AND GSC CONVERTERS FOR THE GRID CONNECTED DFIG DURING TRANSIENT STATE

3.1 Three Phase Symmetrical Faults

The stator voltage will reach zero magnitude during severe three phase's symmetrical fault of very low impedance and stator flux Φ_s gets reduced to zero magnitude. The decay in flux is not as rapid as in voltage and can be explained from the flux decay theorem available in literature and further can be explained as, delay is due to inertial time lag $\tau_s = \frac{L_s}{R_s}$effecting the rotor induced Electromotive Force (EMF) V_{0r}. The flux during fault is given by

$$\Phi_{sf}^s = \Phi_s^s e^{-t/\tau_s} \quad (14)$$

and$\frac{d\Phi_{sf}^s}{dt}$ is negative, indicating its decay. By substituting (14) in (1b)

$$V_{0r}^s = -\frac{L_m}{L_s}(\frac{1}{\tau_s} + j\omega)\Phi_s^s e^{-t/\tau_s} \quad (15)$$

The above equation is converted into a rotor reference frame and neglecting $\frac{1}{\tau_s}$

$$V_{0r}^s = -\frac{L_m}{L_s}(j\omega)\Phi_s^s e^{-j\omega t} \quad (16)$$

By substituting $\Phi_s^s = \frac{V_s^s}{j\omega_s} e^{-j\omega_s t}$in (16)

$$V_{0r}^r = -\frac{L_m}{L_s}(1 - s)V_s \quad (17)$$

$|V_{0r}^r|$is proportional to (1-s)

The converting equation (1a) into the rotor reference frame

$$V_r^r = V_{0r}^r e^{-j\omega t} + R_r i_r^r + \sigma L_r \frac{di_r^r}{dt} \quad (18)$$

Thus rotor equivalent circuit derived from (16) is as shown in Figure 2 [11].

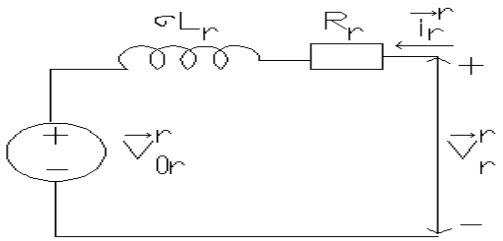

Figure 2. The rotor equivalent circuit

A considerable decrease in pre-fault steady state voltage V_{0r}^r to certain fault voltage during a three phase fault was explained in above analytics. However, RSC converter is designed to meet V_r^r to match V_{0r}^r for rotor current control and the design has to be made for rating of only 35% of stator rated voltage. The voltage dip during fault can be adopted independently or in coordination by using two techniques is explained below.

During fault, at first instant,Φ_s does not fall instantly (16) as shown in the flux and voltage trajectories in Figure 4. If the machine is running at super synchronous speed with slip (s) near to -0.2pu, during fault, rotor speed further increases based on the term (1-s) as given by (16).The above speed change is uncontrollable for a generator having higher electrical and mechanical inertia constants. In order to control the rotor current change, V_r^r has to be increased. Based on the first reason listed above, a voltage $V_{\Phi s}$ has to be injected in the feed forward path for improving the rotor dip to reach to its near steady state value. Converting the equation (16) into a synchronous reference frame and by considering direct alignment of Φ_{ds} with Φ_s we get,

$$V_{\Phi s} = -\frac{L_m}{L_s}\omega\Phi_{ds} \quad (19)$$

The second technique for voltage increase requirement in a rotor is, dip can be compensated by replacing $s\omega_s$ with $(\omega_{\Phi s} - \omega)$ in cross coupling terms $s\omega_s L_r' i_{qr}$ and $s\omega_s L_r' i_{dr}$respectively. The reduction in magnitude and frequency of flux Φ_s, and alignment of flux with the stator voltage without the rate of change in flux angle $\theta_{\Phi s}$ indicates DC offset component in flux.

$$\frac{d\phi_s}{dt} = \omega_{\phi s} = 0 = \omega_f \quad (20)$$

Here, $\omega_f$is the speed of stator flux during fault and this value can be made to zero as offset.

The voltage injection components (20, 21) and compensating components as discussed above are estimated using enhanced flux oriented control (EFOC scheme whose flow chart is shown in Figure 3 and the determined values are incorporated in the RSC controller shown in Figure 1.

$$\frac{d\Theta_{\phi s}}{dt} = \omega_{\phi s} = \frac{V_{\beta s}\phi_{\alpha s} - V_{\alpha s}\phi_{\beta s}}{\phi_{\alpha s}^2 + \phi_{\beta s}^2} = \omega_f \quad (21)$$

When dynamic stability has to be improved, proposed technique controls the decrease in stator and rotor flux magnitude and also damps oscillations at the fault instances. To achieve better performance during transients, this paper proposes a strategy for stator frequency reference to change to zero or other value depending type and severity of disturbance. The accurate measurement of stator and rotor parameters like flux, current helps in achieving better performance during transients. The DC offset stator current reduction

during transients and making the two axis flux and voltage trajectories circular also improves the efficacy of the system performance during any faults. The equations 13 to 18 help in understanding DFIG behaviour during transient conditions and accuracy of its working depends on measurement of rotor current and flux parameters.

3.2 EFOC control technique

The EFOC method of improving field flux oriented control technique helps in improving the performance of the RSC controller of DFIG during fault conditions is described in Figure 4. The DCOC observer does two actions the change in flux values of stationary frame stator references ($\Phi_{\alpha s}, \Phi_{\beta s}$) for tracking radius of trajectory and DCOC for offset change in stationary fluxes ($\Phi_{dc\alpha s}, \Phi_{dc\beta s}$) during fault conditions and controlling them the first action helps in not losing the trajectory from a circle point, and to reach its pre-fault state with the same radius and centre of the circle and hence improving the same rate of flux compensation even during fault without losing stability. The second action helps in controlling and maintaining to nearly zero magnitude using the DCOC technique.

Based on above two actions, if former one is greater with change in trajectory which generally happens during disturbances from an external grid, stator synchronous frequency flux speed ($\omega_{\Phi s}$) changes to synchronous grid frequency flux (ω_s) otherwise $\omega_{\Phi s}$ changes to fault angular frequency value and is injected to RSC voltage control loop as error compensator.

The general form of speed regulation is given by

$$T_e = J\frac{d\omega_r}{dt} + B\omega_r + T_l \tag{22a}$$

$$T_e = (Js + B)\omega_r + T_l \tag{22b}$$

Where T_e is electromagnetic torque, J is moment of inertia and B is friction coefficient, T_l is considered to be disturbance. Multiplying both sides with ω_{error}, we get the equation as

$$T_e\,\omega_{error} = (Js + B)\omega_r\,\omega_{error} + T_l\,\omega_{error} \tag{23}$$

Considering ω_r constant and change in speed error is ω_{error} is control variable, the above equation becomes.

$$P_s^* = (K_{in}s + K_{pn})\,\omega_{error} + P_l \tag{24}$$

As product of torque and speed is power, we will be getting stator reference power and disturbance power as shown below.

$$P_s^* - P_l = (K_{in}s + K_{pn})\omega_{error} \tag{25}$$

Where, $K_{in} = J^*\omega_r$ and $K_{pn} = B^*\omega_r$

Finally direct axis reference voltage can be written by using equation (25) and from Figure 4 is

$$V_{rd}^* = -(\omega_{error})(K_{pn} + \frac{K_{in}}{s}) + (P_s)(K_{pt} + \frac{K_{it}}{s}) \tag{26}$$

$$V_{rq}^* = Q_{error}\,(K_{pQ} + \frac{K_{iQ}}{s}) \tag{27}$$

$$V_{gd}^* = K_{gp}\left(i_{gd}^* - i_{gd}\right) + k_{gi}\int\left(i_{gd}^* - i_{gd}\right)dt - \omega_o L_g i_{gd} + +k_1 V_{sd} \tag{28}$$

$$V_{gq}^* = K_{gp}\left(i_{gq}^* - i_{gq}\right) + k_{gi}\int\left(i_{gq}^* - i_{gq}\right)dt + \omega_o L_g i_{gd} + k_2 V_{sq} \tag{29}$$

$$i_{gq}^* = K_q sqrt(V_{dc}^{2*} - V_{dc}^2) + k_{qi}\int(V_{dc}^* - V_{dc})dt + R_{dc}V_{dc} \tag{30}$$

$$i_{gd}^{*} = K_d \text{sqrt}(V_s^{2*} - V_s^2) + k_{di} \int (V_s^{*} - V_s) dt \quad (31)$$

The rotating direct and quadrature reference voltages of rotor are converted into stationary abc frame parameters by using inverse parks transformation. Slip frequency is used to generate sinusoidal and cosine parameters for inverse parks transformation. In general, during fault and after fault, the DC link voltage across the capacitor at the DFIG back-to-back converter terminal falls and rises, the STATCOM helps in improving the operation and assist in regaining its voltage value respectively to get ready for the operation during next fault. However, STATCOM provides efficient support to the grid-generator system under severe faults by fast action in controlling reactive power flow to grid by maintaining the DC link voltage at the capacitor terminal of DFIG converters constant particularly during transient state. Hence it helps in improving the dynamic stability of the overall system.

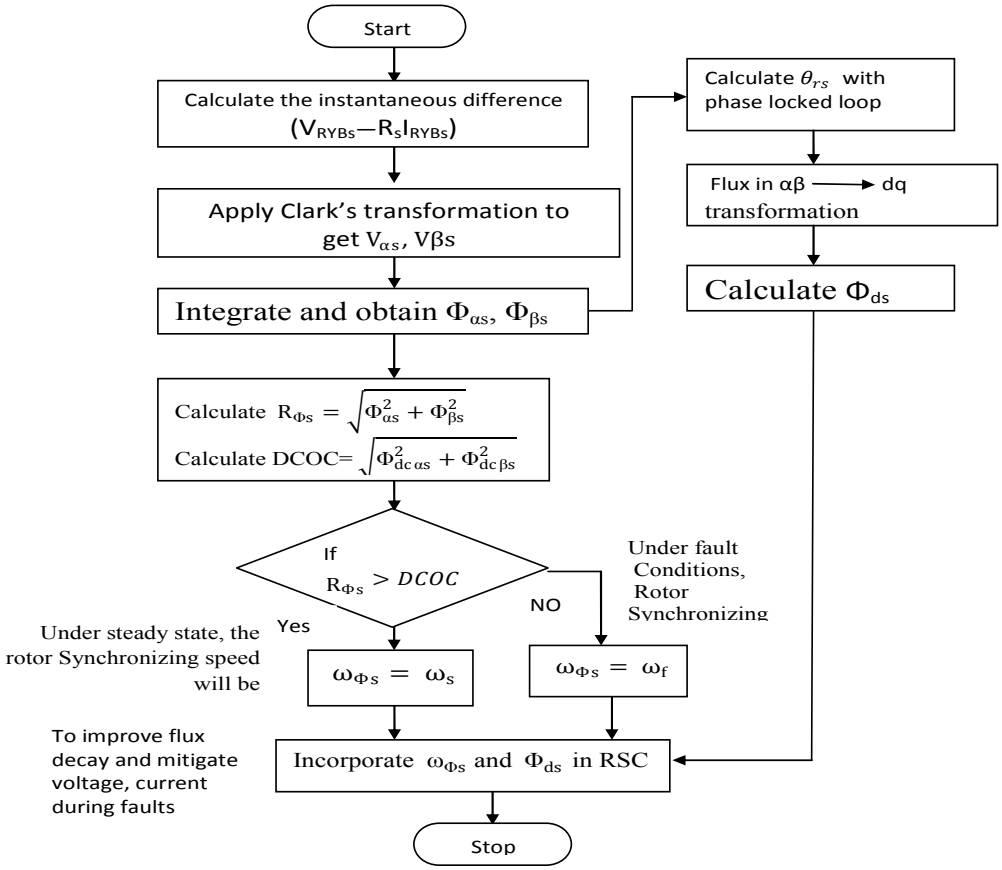

Figure 3. Scheme of enhanced flux oriented control where, DCOC=dc offset component of flux, RΦs=radius of flux trajectory

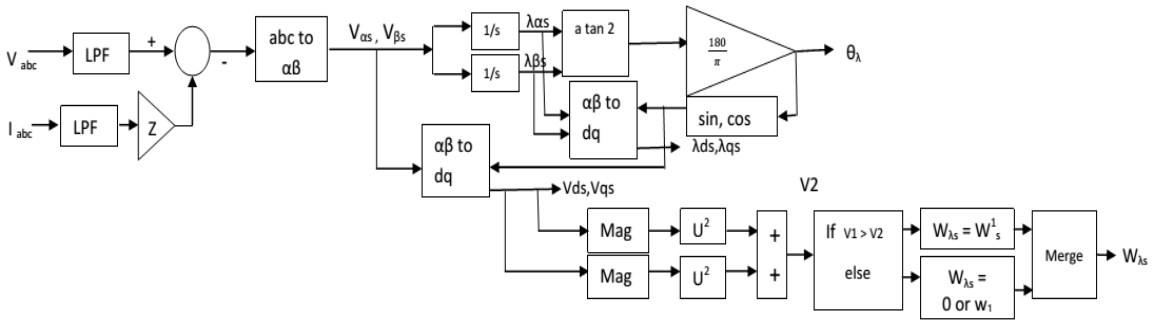

Figure 4. The voltage and current with impedance multiplication are subtracted to get reference voltage

The stator three phase voltages and current are used as inputs for extracting a new arbitrary reference frame for RSC during different fault levels. Here 'z' is the internal resistance of the stator winding. The voltage and current with impedance multiplication are subtracted to get reference voltage as shown in Figure 4. Under normal conditions, the difference will be nearly zero. During fault conditions, the voltage decreases and current increases, which make the difference between these two parameters to the picture. Now the reference three phase voltages are converted to stationary alpha, beta ($V_{\alpha s}$, $V_{\beta s}$) voltages using Clark's transformation. This voltage is integrated and manipulated to get stator flux $\Phi_{\alpha s}$, $\Phi_{\beta s}$. The angle between these two fluxes is flux angle reference θ_{λ}. This angle is used to convert $\Phi_{\alpha s}$, $\Phi_{\beta s}$ to Φ_{ds}, Φ_{qs} and also the two stationary voltages $V_{\alpha s}$, $V_{\beta s}$ are also converted to rotating voltages V_{ds}, V_{qs} using parks transformation. The magnitude of these two voltages is V_2. The reference voltage magnitude of stator is V_1. During normal conditions, V_1 and V_2 are same. But during voltage dips, there exists a difference between the two voltages V_1 and V_2. During faults, if V_1 is greater than V_2, RSC inner control loop and speed reference changes from $W_{\lambda s}$ to W^1s. else in another case, with V_2 greater than V_1, the speed reference varies from $W_{\lambda s}$ to 0 or W_1. Under severe fault, where voltage dip will go beyond the rating of converters, the $W_{\lambda s}$ will be zero. Else it will have certain value specified by flowchart and controller as shown in Figure 3 and Figure 4.

4. DESIGN OF PARAMETERS FOR LITHIUM ION BATTERY

The general layout of DFIG grid connected system is shown in Figure 5a. The design of BESS and capacitor system is shown in Figure 5b [23]. To achieve a dc-bus voltage of 700 V through series connected cells of 12 V, the battery bank should have (600/12) = 50 number of cells in series. Since the storage capacity of this combination is 150 Ah and the total ampere hour required is (600 kW · h/600 V) = 1000 Ah, the number of such sets required to be connected in parallel would be (1000 Ah/150 Ah) = 6.66 or 7 (selected). Thus, the battery bank consists of six parallel-connected sets of 50 series connected battery cells. Thevenin's model is used to describe the energy storage of the battery in which the parallel combination of capacitance (Cb) and resistance (Rb) in series with internal resistance (Rin) and an ideal voltage source of voltage 700 V are used for modelling the battery in which the equivalent capacitance Cb is given as [23]. The value of the BESS parameters is given in the Appendix.

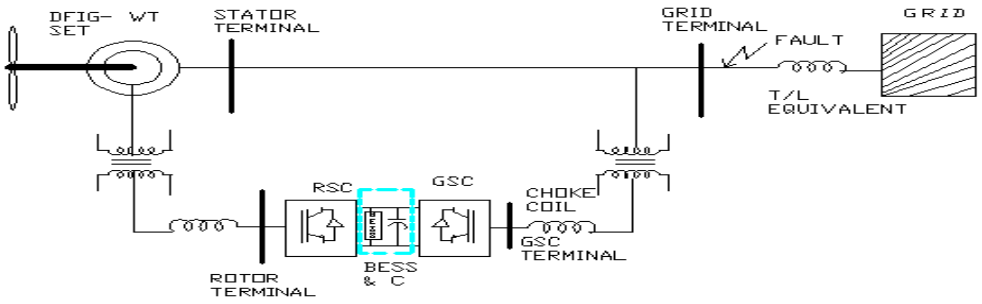

(a)

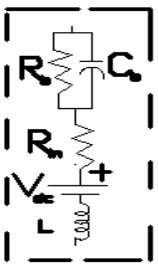

(b)

Figure 5a. Grid connected DFIG showing the location of under-voltage fault, 5(b) BESS system

5. RESULT ANALYSIS

The system under study is shown in Figure 5a. The values are given in the Appendix. A DFIG system is connected directly to grid with RSC and GSC helps in improving reactive power supply to grid. The capacitor at back-to-back converters will provide reactive power to grid in the situations like grid faults

or sudden change in grid terminal voltage. The battery energy storage system (BESS) as in Figure 5b will provide real and reactive power support to the converters to enhance the system operation during grid disturbances. The system performance is studied under two cases. In the first case, efficacy of the system is performance during faults is compared with the work in the literature [8]. A fault occurred at point of common coupling or also called as grid terminal here in Figure 5a. This fault makes the grid and stator voltage to drop to 70% from normal value between 0.15 and 0.5s. In the second case, a comparison is made with out and with battery energy source which is placed between back to back converters of DFIG. In the second case, a fault with resistance of 0.00125Ω between the three phases and ground at PCC occur during 0.8 to 1.2 seconds. The RSC control system is provided with proposed EFOC technique and the GSC control as explained earlier. The need for additional reactive power requirement to maintain voltage profile during faults is due to low power rating of converters.

The performance of an EFOC based test system in Figure 5 with battery energy storage system controller (BESS) is considered for analysis. A total 0.4 seconds three phases to ground fault occurred at PCC is considered for the study with fault resistance of 0.0015Ω. During fault, stator voltage decreased from 1pu to 0.6pu with a 40% decrease compared to normal during 0.1 to 0.5 seconds as shown in Figure 6(a). The decrease in grid voltage during fault depends mainly on location, fault resistance and type of fault. The efficacy of the proposed EFOC system can be compared with [9-13, 21 and 22] for the operation and reactive power control during faults.

The stator current is nearly constant with 0.8pu at healthy conditions to 0.56pu during fault and regains instantly without surges, its normal value once fault is cleared as in Figure 6(b). Due to unpredictable surge current entering into the system, at fault instant, there will be current surges. But due to faster action of controllers, this surge current is limited. The surges at these instants are due to sudden change in capacitor voltage at the back to back converters and also due to a sudden inrush of fault current into the stator and rotor windings. The rotor current in Figure 8(c) which is initially under steady state without fault is 0.70pu. There is a very small surge current in the rotor at fault instant making the current to increase and then decreased and maintained at 0.50pu from 0.1 to 0.3s. This current has a decrease in magnitude during fault, but no change in rotor slip frequency because of the proposed control scheme. It reached its pre-fault value after the fault is cleared. From the equations (15-18), with the change in the stator and rotor flux linkage value and rotor slip, the rotor voltage increases slightly exponentially to certain value because of change in back emf of DFIG. Because of this, based on Figure 3, it can be observed that rotor current, thereby stator current will decrease with a proposed scheme instead of increasing during a fault. The rotor voltage is almost constant at 0.4pu before, during and after fault is shown in Figure 8(d).

Case 1: Comparison for the work with 70% decrease in grid voltage

In this case, much severe fault occurred at PCC near grid, which makes the grid voltage decreased to 0.3pu from 1pu during 0.1 to 0.5s. This decrease is 70% for stator voltage compared to rated voltage under healthy conditions as shown in Figure 6 (a). Because of this fault, the stator and rotor current surges are produced at the instant of fault at 0.1s. After 0.012s, these currents decreased and reached a smaller and safe value with the proposed technique. The stator current in Figure 6(b) which is initially 0.80pu before fault, reaches to 0.4pu during fault between 0.1 and 0.3s. A surge current of magnitude 1.5pu is produced at fault instant 0.1s and lasts for one cycle. Compared to the work in literature [8,26], the offset DC components (DCOC) in flux during fault are minimised even with severe fault with a fault resistance of 0.00125Ω. The decrease in DC offsets current oscillations, limiting surge currents, maintaining current waveform, all are considered advantages with proposed EFOC. A steady state is reached and stator current maintained as in pre-fault state. With EFOC technique, continuity of current, thereby power flow is improved. The overall system stability and performance are improved. The results obtained with BESS which is placed between the back to back converters across normal capacitor, helps to realize faster control action with sustained oscillations and the EFOC limits the decoupled current control parameters. This BESS helps in sustaining the system without much severe oscillations due to severe faults with the additional real power support from battery and reactive power from semi-conductor switches.

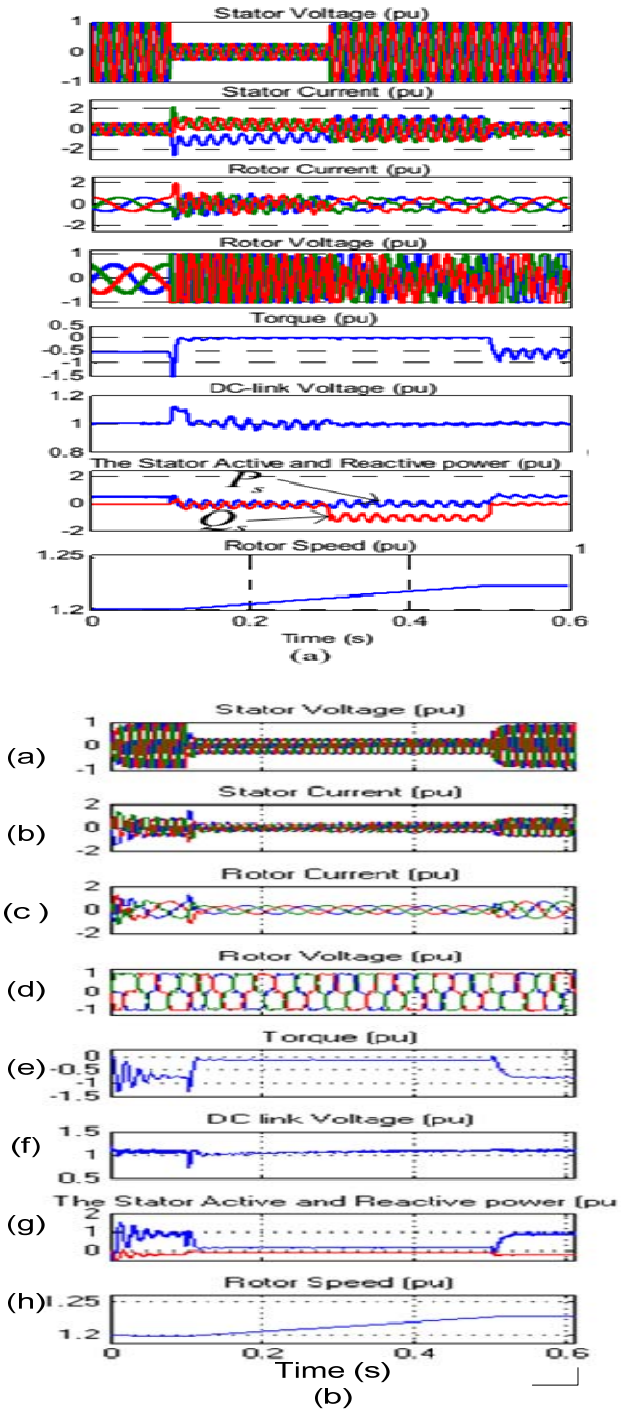

Figure 6a, waveforms snapshot from reference [3] and Figure 6b Performance of DFIG with 40% dip in grid voltage with EFOC (a) stator voltage, (b) stator current, (c) rotor current, (d) rotor voltage, (e) actual electromagnetic torque, (f) DC link voltage across capacitor at back to back converters (g) stator real and reactive power, (h) rotor speed

The rotor current decreased from 0.70pu to 0.3pu during fault and regained to 0.7pu after the fault is cleared as shown in Figure 6(c). The frequency of rotor waveform is constant during this fault. With proper switching control action by RSC and GSC ensures the system sustaining capability by limiting the surge current. The proposed RSC control technique with optimal speed reference control scheme, flux decay control and improved demagnetisation control action makes the rotor current not to increase naturally during a fault. Without the need for any external real or reactive power sources or crowbar arrangement and with the

same converter rating, the rotor and stator current surge control is possible. Compared to work in [8] and [26], the distortions in the rotor and stator parameters are very less with the proposed control scheme. The rotor voltage is almost constant during and after the fault with the proposed control action. The rotor voltage is also almost constant at 0.40pu as shown in Figure 6 (d).

The EMT at fault instant 0.1s has surged -1.4pu and reaches a steady value during fault to -0.1pu at 0.105s is shown in Figure 6(e). Later, when the fault is cleared, reaches a steady state value at 0.3s at fault clearing as shown here. With the results in [8], the EMT oscillations after fault lasts for mare than 0.1s as shown in Figure 11. With a proposed EFOC technique with BESS, the torque oscillations are eliminated and stability was improved.

The DC voltage in Figure 6(f) at converters is maintained constant at 1.0 pu during and after fault without oscillations. A sag up to 0pu volts at fault instant 0.1s in DC voltage dip is observed at fault instant, due to unexpected occurance of fault. With fast acting control strategy, the voltage dip can get mitigated. Even if fault exists for more than 0.5s time period, the system can sustain stability as DC capacitance voltage is maintained constant at back-to-back converters. The DC capacitor rating at back-to-back converters will also play a vital role in storing and delivering this excess current during the faults. The GSC circuit, helps in controlling the decay in DC link voltage, thereby overall stability is improved.

The stator real and reactive powers are shown in Figure 6(g). Before the fault occurrence, the stator real power is 0.98pu, during a fault, it reached to 0.13pu between 0.1 to 0.3s and regain to pre-fault value once fault is cleared. Similarly, the reactive power changed from 0pu to 0.18pu during fault and reaches -0.02pu after the fault is cleared. It can be observed that, there are no oscillations in real and reactive power and hence there are no distortions in the voltage or current waveforms. The rotor speed is maintained nearly constant during this type of severe fault. The rotor speed increases to 1.214pu as shown in Figure 6(h) and reaches steady state once fault is cleared.

Case 2: Comparison of system performance without and with BESS for 70% decrease in grid voltage

The grid voltage and current waveforms without and with BESS is shown in Figure 7a (i) and (ii). In this, grid waveforms are nearly constant with voltage dropping from 1pu to 0.45pu during fault. It again regains to pre-fault voltage level once fault was cleared and system was restored. The current waveforms without, sub-transient waveform is taking more time to settle without BESS than with BESS.

The stator 3ϕ voltage and current waveforms without and with BESS is shown in Figure 7b (i) and (ii). In general without fault, the stator voltage and current are 1 per-unit (pu). When a three phase symmetrical fault of 0.005Ω occur at point of common coupling (PCC), voltage dropped to 0.89pu without BESS and current dropped to 0.55pu. With proposed EFOC technique, the drop in voltage and current are to a smaller value compared to the reference [2, 4, 5 and 8]. For same system, with external DC supply using (BESS) battery equivalent source, drop in voltage is controlled and maintained constant at 1.0pu. The stator current remained nearly same as the system without BESS. The use of BESS helps in supplying additional active and reactive power supply to the converters which helps in improving stator voltage profile during faults. But the grid voltage declined from 1pu to 0.45pu, but still stator voltage and current are maintaining better voltage profile of nearly 0.9pu and current of 0.55pu.

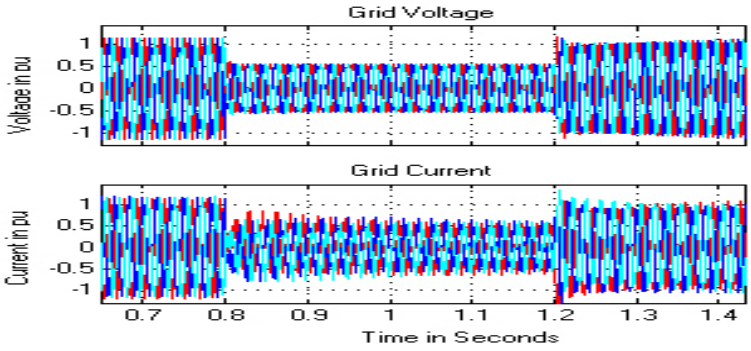

Figure 7a. (i) grid voltage and current without BESS

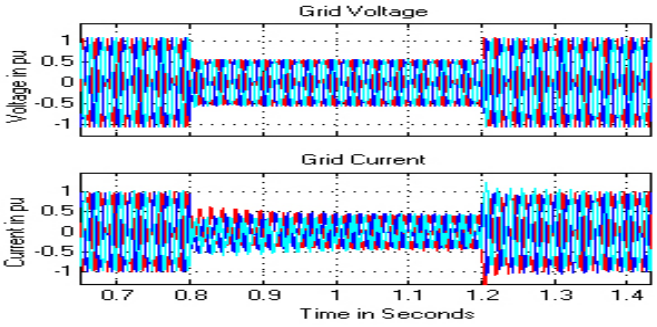

Figure 7a. (ii) with BESS

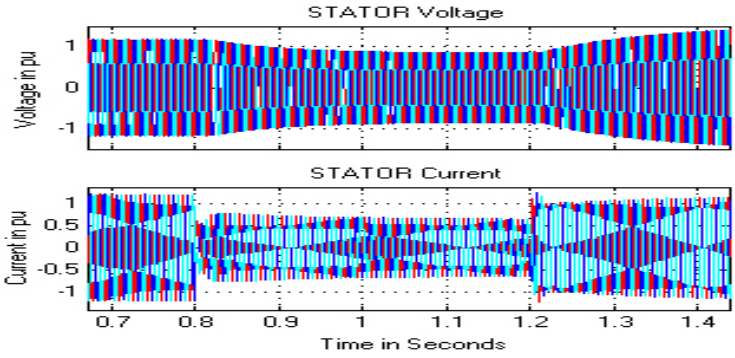

Figure 7b. (i) stator voltage and current without BESS

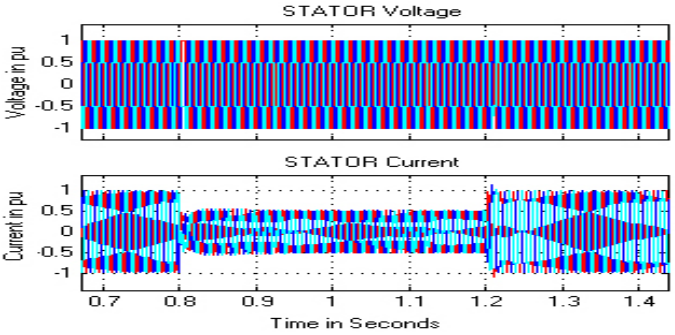

Figure 7b. (ii) with BESS

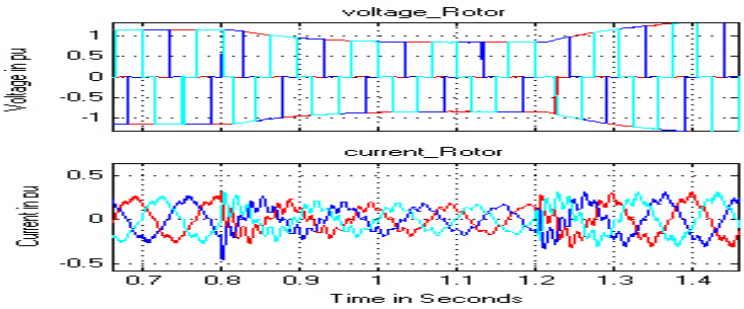

Figure 7c. (i) rotor voltage and current without BESS

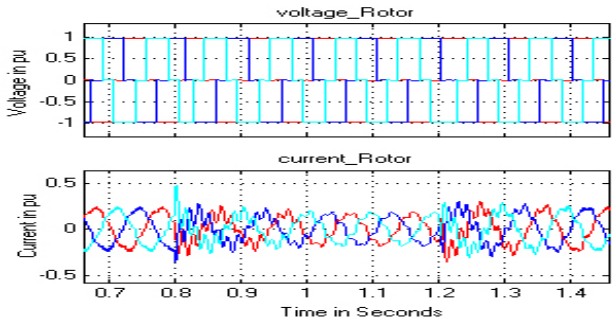

Figure 7c. (ii) with BESS

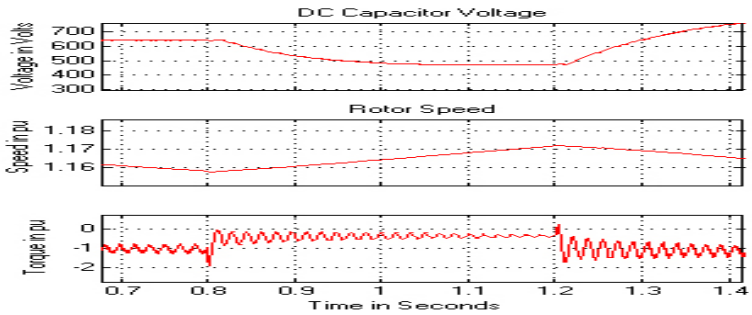

Figure 7d. (i) Generator parameters without BESS

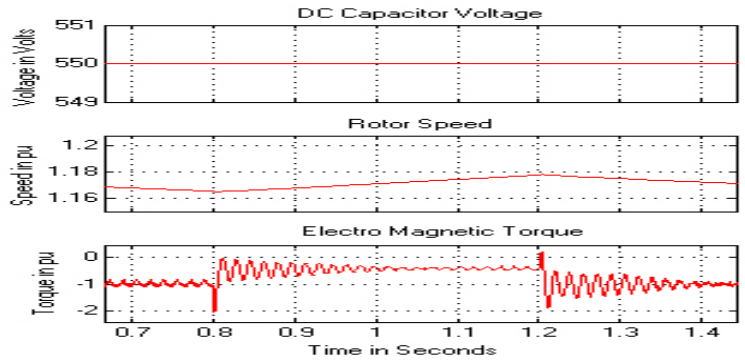

Figure 7d. (ii) with BESS

Figure 7. Stator, rotor winding and grid voltage and current waveforms and machine parameters when a symmetrical fault occurs between 0.8-1.2s with (i) without BESS and (ii) with BESS

The Figure 7c (i) and (ii) show the rotor voltage and current waveforms without and with BESS and EFOC based control strategy. Before fault, rotor voltage and current are at 1pu and 0.25pu. When fault occurred at 0.8s, the rotor voltage decreased to 0.9pu and current with small distortions at the beginning decreased to 0.2pu with EFOC. The improvement in current profile during faults and maintaining current and voltage profile is due to the control in flux decay as explained in section 3.2. Compared to the output waveforms from literature [2, 3, 4 and 5], the proposed strategy helps in not only improving rotor and stator current profile and also mitigating distortion [2, 3 and 5] in current waveforms during faults. The rotor waveform with BESS is shown in Figure 7c (ii). The voltage profile is maintained constant during and after fault just like system in pre-fault state. The rotor current waveforms are having much lesser distortions and settles in settles in less than 2 cycles during fault as without BESS with 3 cycles (Blue phase current waveform).

The DFIG converters common DC link voltage, output rotor speed and electromagnetic torque without BESS and with BESS for proposed strategy is shown in Figure 7d (i) and (ii). With capacitor as DC

source as in Figure 7d (i), the voltage decreased from 620 volts to 480V during 0.8 to 1.2 seconds and increased to 720V at 1.5s and slowly decreased and maintained to 620V from 1.8s. This sudden increase in DC link voltage is due to sudden clearance of fault and rapid increase in PCC voltage. In general, grid system is much stronger than a DFIG or a single power plant based system. The sudden change in overall impedance of the system after fault, change in direction of current flow in RSC current and sudden decrease in reactive power requirement make the DC link voltage to increase and then to maintain as before fault. With [2, 3], the DC link voltage increased to a much higher value than our proposed system. The rotor speed remained nearly constant during fault with EFOC. The rotor speed changed from 1.16pu to 1.17 during fault and reaches to 1.58pu at 1.5s and reaches 1.16 and maintained constant without BESS based system. With penetrations in wind turbine, the DFIG system will have small fluctuations in electromagnetic torque (EMT) during steady state. The EMT decreased from 1pu in magnitude to -0.4pu during fault and regained to -1pu when fault cleared at 1.2pu.

6. CONCLUSION

A conventional DFIG wind turbine system connected to the grid was considered in the analysis. A three phase fault is imagined to occur at PCC between 0.1 and 0.3 seconds, making the grid voltage to decrease to 30% and 70% compared to normal. With the proposed EFOC technique, rotor current during fault is maintained at certain value without increasing or getting zero. The stator and rotor current dip is observed with proposed control scheme. The waveforms are sinusoidal without DC offset components and the system is maintained synchronism at 70% dip in the voltage. The reduction in torque is observed at 70% dip in grid voltage, but regained to normal value without oscillations after the fault is cleared. The rotor speed is constant without much swell during severe fault with the proposed control scheme. The overall secured operation can be guaranteed during and the fault with proposed EFOC technique. The torque ruipple and surges in current waveform possible with the help of a fuzzy controller, as it is a fatsre device than a conventional PI controller.The post fault recovery in machine voltage and current waveforms have taken place without any surges.

The wind energy conversion system with good LVRT technique will ensure dynamic stability by complying with modern wind grid codes. A DFIG wind turbine system to limit transient over currents in rotor circuit is achieved by using advanced EFOC algorithmic technique. With proposed technique, usage of crowbar circuit can be eliminated. A comparison is made without and with an external BESS with a symmetrical fault occurring at PCC. With proposed technique, the overall dynamic response of the system is improved by suppressing not only fault transient but also post fault transients. This methodology enhances the lethargic system to reach its steady state at an improved rate, thus providing good quality as well as reliable power with the aid of BESS.

The effectiveness of the proposed technique analyses the comparison between without and with BESS for DC link capacitor voltage. The rotor speed and electromagnetic torque during and after three phase symmetrical faults were improved to a better level after introducing BESS. It is observed that with grid voltage drop to 50%, the stator and rotor voltages are still maintaining at 80% dip during fault. It is maintaining nearly constant voltage profile with BESS. The stator and rotor current waveforms preserve seamless during the fault without and with BESS. There is a very small dip in the generator winding currents during fault and reached steady state immediately after the fault was relieved. The capacitor voltage dip is also from 620 to 480V during fault with EFOC technique. The rotor speed in both cases maintained nearly constant between 1.16 to 1.18pu. The EMT is not getting zero, but is maintained at 0.4pu magnitude during fault. The ripples in EMT were reduced with BESS than capacitor alone system. The overall system performance during severe symmetrical fault can be improved using EFOC technique and further improvement can be made if BESS is incorporated in the DC link of the converters.

Appendix

The parameters of DFIG used in simulation are,

Rated Power = 1.5MW, Rated Voltage = 690V, Stator Resistance Rs = 0.0049pu, rotor Resistance Rr = 0.0049pu, Stator Leakage Inductance Lls = 0.093pu, Rotor Leakage inductance Llr1 = 0.1pu, Inertia constant = 4.54pu, Number of poles = 4, Mutual Inductance Lm = 3.39 pu, DC link Voltage = 415V, Dc link capacitance = 0.2F, Wind speed = 14 m/sec.

Grid Voltage = 25 KV, Grid frequency = 60 Hz, Grid side Filter: Rfg = 0.3Ω, Lfg = 0.6nH, Rotor side filter: Rfr = 0.3mΩ, Lfr = 0.6nH, Battery Specifications: Cb = 180000 F, Rb = 10 kΩ, Rin = 0.2 Ω, Vocmax = 620 V, Vocmin = 500 V, Storage = 600 kW · h, L = 1 mH.

REFERENCES

[1] Wang Yun; Zhao Dong-li; Zhao Bin; Xu Hong-hua, "*A Review of Research Status on LVRT Technology in Doubly-fed Wind Turbine Generator System*", Proc. on ICECE, 2010, pp: 4948 – 4953.

[2] Rongwu Zhu, Zhe Chen, Xiaojie Wu, and Fujin Deng, "Virtual Damping Flux-Based LVRT Control for DFIG-Based Wind Turbine", *IEEE Transactions On Energy Conversion*, Vol. 30, No. 2, June 2015, pp. 714-725.

[3] Dong liang Xie; Zhao Xu; Lihui Yang; Ostergaard, J.; Yusheng Xue; Kit Po Wong, "A Comprehensive LVRT Control Strategy for DFIG Wind Turbines With Enhanced Reactive Power Support", *IEEE Transactions on Power Systems*, Volume: 28 ,2013 , pp: 3302 – 3310.

[4] Lihui Yang; Zhao Xu; Ostergaard, J.; Zhao Yang Dong; Kit Po Wong, "Advanced Control Strategy of DFIG Wind Turbines for Power System Fault Ride Through", *IEEE Transactions on Power Systems*, Volume: 27 , Issue: 2,2012 , Pp: 713 – 722.

[5] Rahimi, M.; Parniani, M., "Efficient control scheme of wind turbines with doubly fed induction generators for low-voltage ride-through capability enhancement", *IET Renewable Power Generation*, Vol. 4 , No. 3, 2010 , pp: 242 – 252.

[6] Jiaqi Liang; Howard, D.F.; Restrepo, J.A.; Harley, R.G., "Feedforward Transient Compensation Control for DFIG Wind Turbines During Both Balanced and Unbalanced Grid Disturbances", *IEEE Transactions on Industry Applications*, Volume: 49 , Issue: 3, 2013 , pp: 1452 – 1463

[7] Jiaqi Liang; Wei Qiao; Harley, R.G., "Feed-Forward Transient Current Control for Low-Voltage Ride-Through Enhancement of DFIG Wind Turbines", *IEEE Transactions on Energy Conversion*, Vol. 25 , No. 3, 2010, pp: 836 – 843.

[8] Shuai Xiao; Geng Yang; Honglin Zhou; Hua Geng, "An LVRT Control Strategy Based on Flux Linkage Tracking for DFIG-Based WECS", IEEE Transactions on Industrial Electronics, Volume: 60 , Issue: 7, 2013 , Pp: 2820 – 2832.

[9] Vrionis, T.D.; Koutiva, X.I.; Vovos, N.A., "A Genetic Algorithm-Based Low Voltage Ride-Through Control Strategy for Grid Connected Doubly Fed Induction Wind Generators", *IEEE Transactions on Power Systems*, Vol. 29, 2014, pp: 1325 – 1334.

[10] da Costa, J.P.; Pinheiro, H.; Degner, T.; Arnold, G., "Robust Controller for DFIGs of Grid-Connected Wind Turbines", *IEEE Transactions on Industrial Electronics*, Vol. 58 , No. 9 2011 , pp: 4023-4038.

[11] Vidal, J.; Abad, G.; Arza, J.; Aurtenechea, S., "Single-Phase DC Crowbar Topologies for Low Voltage Ride Through Fulfillment of High-Power Doubly Fed Induction Generator-Based Wind Turbines", *IEEE Transactions on Energy Conversion*, Vol. 28 , No. 3, 2013 , pp: 768-781.

[12] Abbey, C.; Joos, G., "Super-capacitor Energy Storage for Wind Energy Applications", *IEEE Transactions on Industry Applications*, Vol. 43 , No. 3 : 2007 , pp: 769-776.

[13] Guo, W.; Xiao, L.; Dai, S.; Li, Y.; Xu, X.; Zhou, W.; Li, L,"LVRT Capability Enhancement of DFIG With Switch-Type Fault Current Limiter", *IEEE Transactions on Industrial Electronics*, Vol. 62 , No. 1, 2015 , pp: 332-342.

[14] Wenyong Guo; Liye Xiao; Shaotao Dai, "Enhancing Low-Voltage Ride-Through Capability and Smoothing Output Power of DFIG With a Superconducting Fault-Current Limiter–Magnetic Energy Storage System", *IEEE Transactions on Energy Conversion*, Vol. 27, No. 2, 2012 , pp: 277 – 295.

[15] X.Y. Wang, D. Mahinda Vilathgamuwa, and S.S. Choi, "Determination of Battery Storage Capacity in Energy Buffer for Wind Farm", *IEEE Transactions on Energy Conversion*, Vol. 23, No. 3, September 2008, pp: 868-878.

[16] Minsoo Jang, Mihai Ciobotaru, and Vassilios G. Agelidis, "A Single-Phase Grid-Connected Fuel Cell System Based on a Boost-Inverter", *IEEE Transactions on Power Electronics*, Vol. 28, No. 1, January 2013, pp: 279-288.

[17] Quanyuan Jiang, Yuzhong Gong, and Haijiao Wang, "A Battery Energy Storage System Dual-Layer Control Strategy for Mitigating Wind Farm Fluctuations", *IEEE Transactions on Power Systems*, Vol. 28, No. 3, August 2013, p. 3263-3273.

[18] Xiaoyu Wang, Meng Yue, Eduard Muljadi and Wenzhong Gao, "Probabilistic Approach for Power Capacity Specification of Wind Energy Storage Systems", *IEEE Transactions on Industry Applications*, Vol. 50, No. 2, March/April 2014, pp. 1215-1224.

[19] Bhim Singh, and Shailendra Sharma, "Stand-Alone Single-Phase Power Generation Employing a Three-Phase Isolated Asynchronous Generator", *IEEE Transactions on Industry Applications*, Vol. 48, No. 6, November/December 2012, pp. 2414-2423.

[20] Ioan Serban, and Corneliu Marinescu, "Control Strategy of Three-Phase Battery Energy Storage Systems for Frequency Support in Microgrids and with Uninterrupted Supply of Local Loads", IEEE Transactions on Power Electronics, Vol. 29, No. 9, September 2014, pp. 5010-5020.

[21] Laxman Maharjan, Tsukasa Yamagishi, Hirofumi Akagi, and Jun Asakura", Fault-Tolerant Operation of a Battery-Energy-Storage System Based on a Multilevel Cascade PWM Converter With Star Configuration", *IEEE Transactions on Power Electronics*, Vol. 25, No. 9, September 2010, pp: 2386-2396.

[22] Michail Vasiladiotis, and Alfred Rufer, "Analysis and Control of Modular Multilevel Converters With Integrated Battery Energy Storage", *IEEE Transactions on Power Electronics*, Vol. 30, No. 1, January 2015, Pp. 163-175.

[23] Puneet K. Goel, Bhim Singh, S. S. Murthy, Navin Kishore, "Isolated Wind–Hydro Hybrid System Using Cage Generators and Battery Storage", *IEEE Transactions on Industrial Electronics*, Vol. 58, No. 4, April 2011, pp. 1141-1153.

[24] Weissbach. R. S, Karady. G. G, Farmer. R. G, "A combined uninterruptible power supply and dynamic voltage compensator using a flywheel energy storage system", *IEEE Transactions on Power Delivery*, Vol. 16, pp. 265-270, Apr 2001.

[25] Doria Cerezo. A, "Control and performance of a doubly-fed induction machine intended for a flywheel energy storage system", *IEEE Transactions on Power Electronics*, vol. 28, pp. 605-606, Jan 2013.
[26] Murthy, K. Viswanadha S., M. Kirankumar, and G. R. K. Murthy. "A performance comparison of DFIG using power transfer matrix and direct power control techniques." *International Journal of Power Electronics and Drive Systems (IJPEDS)*, Vol 5., No.2, 2014, pp. 176-184.
[27] Nora, Zerzouri, and Labar Hocine. "Active and Reactive Power Control of a Doubly Fed Induction Generator." *International Journal of Power Electronics and Drive Systems (IJPEDS)*, Vol 5, No. 2, 2014, pp. 244-251.
[28] Gopala, Venu Madhav, and Y. P. Obulesu. "A New Hybrid Artificial Neural Network Based Control of Doubly Fed Induction Generator." *International Journal of Electrical and Computer Engineering (IJECE)*, vol. 5, No. 3, 2015, pp. 379-390.
[29] Madhav, G. Venu, and Y. P. Obulesu. "A Fuzzy Logic Control Strategy for Doubly Fed Induction Generator for Improved Performance under Faulty Operating Conditions." *International Journal of Power Electronics and Drive Systems (IJPEDS)*, Vol. 4, No.4, 2014, pp. 419-429.
[30] Boulahia, Abdelmalek, Mehdi Adel, and Hocine Benalla. "Predictive Power Control of Grid and Rotor Side converters in Doubly Fed Induction Generators Based Wind Turbine." *Bulletin of Electrical Engineering and Informatics*, Vol. 2, No. 4, 2013, pp. 258-264.
[31] Sireesha, K. L., and G. Kesava Rao. "Droop Characteristics of Doubly Fed Induction Generator Energy Storage Systems within Micro Grids." *International Journal of Power Electronics and Drive Systems (IJPEDS)*, Vol. 6, No. 3, 2015, pp. 429-432.

BIOGRAPHIES OF AUTHORS

D.V.N. Ananth was born in Visakhapatnam, India on 20th August 1984. He received B.Tech Electrical Engineering from Raghu Engineering College, Visakhapatnam and M.Tech from Sreenidhi Institute of Science & Technology, Hyderabad, India. He is working as an Assistant Professor in VITAM College of Engineering in Electrical Department since December 2010. He is currently working towards his PhD degree from GITAM University, Visakhapatnam His favorite topics include Renewable energy resources, DFIG, industrial drives, power systems, power electronics, control systems, HVDC and Reactive power compensation techniques. His contact address is nagaananth@gmail.com

Dr. G.V. Nagesh Kumar was born in Visakhapatnam, India in 1977. He graduated College of Engineering, Gandhi Institute of Technology and Management, Visakhapatnam, India, Masters Degree from the College of Engineering, Andhra University, Visakhapatnam. He received his Doctoral degree from Jawaharlal Nehru Technological University, Hyderabad. He is presently working as Associate Professor in the Department of Electrical and Electronics Engineering, GITAM University, Visakhapatnam. His researches interests include gas insulated substations, fuzzy logic and neural network applications, distributed generation, Partial Discharge Studies and Bearingless drives. He has published 102 research papers in national and international conferences and journals. He received "Sastra Award", "Best Paper Award" and "Best Researcher Award". He is a member of various societies, ISTE, IEEE, IE and System Society of India. He is also a reviewer for IEEE Transactions on Dielectrics and Electrical Insulation, Power Systems and a member on Board of several conferences and journals.